

## A Study on Effective Temperature of CSBA-loaded UO<sub>2</sub> Fuel Pellet

Anisur Rahman, Xuan Ha Nguyen, Yonghee Kim\*  
Korea Advanced Institute of Science and Technology (KAIST)  
291 Daehak-ro, Yuseong-gu, Daejeon, 34141, Republic of Korea  
\*Corresponding author: yongheekim@kaist.ac.kr

### 1. Introduction

The determination of fuel temperature is important for improved nuclear reactor design and safety analysis. Many studies have focused on determination of the temperature of the UO<sub>2</sub> fuel rod. Goltsev A.O. et al. and Rowlands, G. calculate the effective temperature of the UO<sub>2</sub> fuel rod using non-uniform radial temperature profile [1, 2]. They recommended error can be eliminated by performing calculations that take into account the actual temperature distribution. Recently, a conceptually innovative BA design, centrally-shielded burnable absorber (CSBA), was proposed [3]. CSBA is a typical PWR UO<sub>2</sub> pellet loaded with lumped BA in its centerline, which can offer highly neutronics feasibility to achieve a soluble boron free system. As the temperature profile of the CSBA design fuel is different from that of conventional fuel, it is required to evaluate the temperature distribution of the CSBA fuel rod.

In this paper, Finite Element Method (FEM) was developed to determine the temperature distribution within the CSBA fuel pellet, while the power distribution of the fuel pellet was updated from Monte Carlo Serpent 2 code [4]. An iterative procedure was used to couple between FEM and Serpent codes in order to obtain detailed temperature profiles. Subsequently, the effective temperature of the fuel pellet can be calculated by using Serpent 2 with the detailed temperature profile, so that the reactivity found from detailed temperature distribution of the fuel pellet is preserved with the use of effective temperature.

### 2. CSBA Design

CSBA fuel rod is most like a typical PWR UO<sub>2</sub> pellet and spherical balls lumped gadolinia inside the fuel pellet. Gadolinia enhances the neutronic spatial self-shielding and reduce its depletion rate in a thermal spectrum. In order to adjust gadolinia's self-shielding properties and the resulting burnup-dependent consumption, the burnable absorber can be split into two or three equi-volume balls inside the same pellet with symmetrically axial-wise. Therefore the self-shielding and burnup-dependent consumption properties reduce the excess reactivity and active control of the reactor.

In this paper, a single fuel pellet with two 0.1 cm radius gadolinia balls putted symmetrically centerline was chosen to calculate the effective temperature of the pellet. Because this design is mostly used in the CSBA-loaded core. The pellet and gadolinia balls were split into 5 equi-volume cell as shown in Fig. 1 and Table 1 shows the specifications of the fuel pellet. The power density and

UO<sub>2</sub> density of the CSBA fuel rod are 25.99 W/gU and 10.4668 g/cm<sup>3</sup>, respectively. Ring-wise power distributions of the fuel pellet were calculated at different stage of fuel burnup. As the burnable absorber inside the fuel rod thus the temperature distribution of CSBA fuel rod will be quite different from that of a conventional UO<sub>2</sub> fuel rod.

Table1: Fuel pellet design parameters

Parameters	Value
UO <sub>2</sub> pellet height (cm)	1.00
UO <sub>2</sub> pellet radius (cm)	0.40958
Clad inner radius(cm)	0.41873
Clad outer radius (cm)	0.47600
CSBA ball radius (cm)	0.1
Number of CSBA ball	2

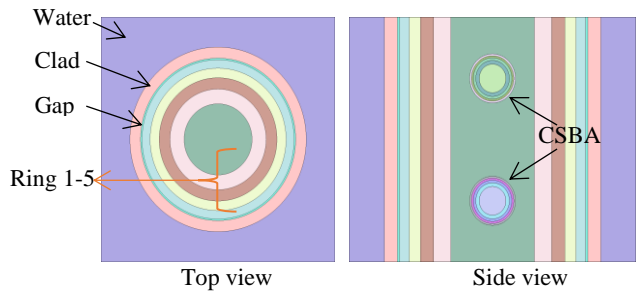


Fig. 1: CSBA-loaded fuel pellet.

### 2. Methodology

The Galerkin method for the axisymmetric [5] was applied to solve the heat conduction problem in order to determine the real temperature distribution of CSBA fuel pellet. The steady state heat conduction equation can be written as integral form:

$$\int_{\Omega} N_i \left[ \lambda_r \frac{\partial}{\partial r} \left( r \frac{\partial T}{\partial r} \right) + \lambda_z \frac{\partial^2 T}{\partial z^2} + G \right] = 0 \quad (1)$$

The spatial approximation result in the familiar final form of the matrix equation is written as:

$$[K]\{T\} = \{f\}_e$$

Where,

\{T\} = Temperature matrix

$$[K] = \int_{\Omega} [B]^T [D] [B] d\Omega + \int_{\Gamma} h [N]^T [N] d\Gamma$$

$$\{f\}_e = \int_{\Omega} G [N]^T r_e d\Omega - \int_{\Gamma_q} q [N]^T r_e d\Gamma + \int_{\Gamma_h} h T_a [N]^T r_e d\Gamma$$

The fuel pellet geometric problem is a three dimensional but a geometric symmetry about a radially axis and all field functions are independent of the circumferential direction ( $\theta$  direction). Then, the domain can be represented by axisymmetric ring elements, and analyzed in a similar fashion to that of a two-dimensional problem. A two dimensional triangular mesh was created by the COMSOL multi-physics as shown in Fig. 2.

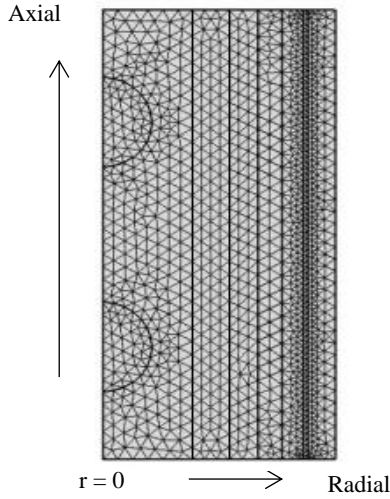


Fig. 2: Two-dimensional meshing of a pellet

Temperature- and burnup-dependent thermal conductivity, as shown in Fig. 3, was used to solve heat conduction problem. Also the thermal conductivity used for clad and gadolinia is shown in Fig. 4. Furthermore tabulated burnup-dependent heat transfer coefficient of  $UO_2$  fuel to cladding material, as shown in Fig. 5, was used to calculate the thermal conductivity of the fuel gap.

The volume-average temperature  $\bar{T}$  of the fuel rod is defined as:

$$\bar{T} = \frac{\int T(r) \cdot dV}{\int dV} \quad (2)$$

where  $T(r)$  is obtained from thermal hydraulic throughout the entire unit cell

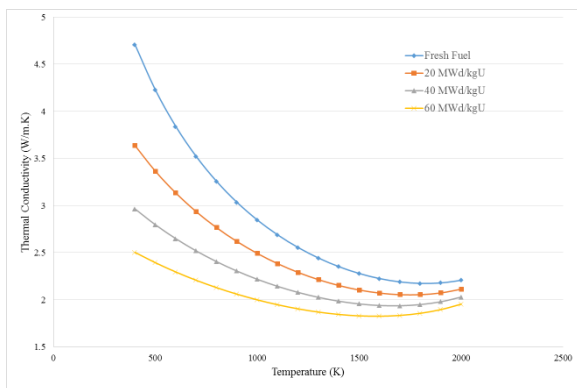


Fig. 3: Burnup-dependent thermal conductivity of  $UO_2$

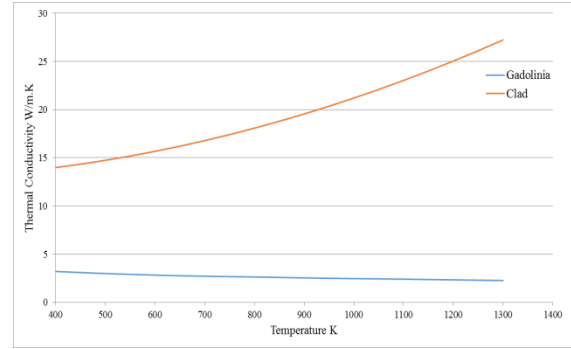


Fig. 4: Thermal conductivity of Clad and Gadolinia.

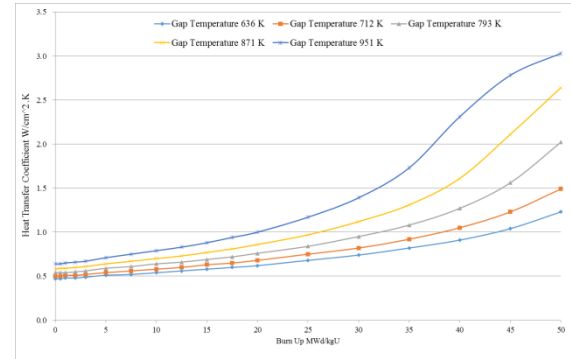


Fig. 5: Burnup-dependent heat transfer coefficient between fuel and clad.

The detailed and volume-average temperature distribution were calculated from the FEM thermal hydraulic analysis of the fuel pellet. In order to obtain the reference values, the Serpent neutronic calculation coupled with FEM thermal hydraulics analysis was performed until convergence. The effective temperature of the fuel pellet was then calculated to preserve the total reactivity found from the detail temperature distribution.

#### 4. Numerical Results and Discussion

The ring-wise temperature distribution were calculated using power distributions obtained from Monte Carlo Code Serpent, which is shown in Fig. 6. It is noted that, in Serpent calculation, the number of histories is 100,000 with 1000 active and 100 inactive cycles, resulting in 6.5 pcm of  $k_{inf}$  uncertainty. From the figure, it is clear to see that Rim effect is enhanced in the periphery region when the fuel burnup increases. The ring-wise and volume-average temperatures at every single stage of burnup is shown in Fig. 7. The ring 1 temperature increases with burnup as power distribution increases, due to fast depletion of gadolinia in ring 1. At high burnup condition, the temperature of the outermost ring decreases as a result of significant increase in gap heat transfer coefficient, even the power is enhanced by Rim effect. On the other hand, the volume-average temperature of CSBA pellet, around 850K, is lower than that of PWR pellet, about 950 K. It is due to a low power density of 25.99 W/gU

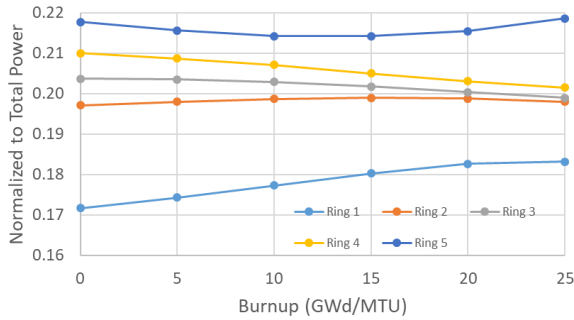


Fig. 6: Ring-wise power distribution at different burnup conditions.

The effective temperatures of the fuel pellet at different burnup were iteratively calculated by using Serpent. Table 2 indicates the comparison between the infinite multiplication factors of volume-average, effective temperatures and reference temperature distribution of the fuel pellet. It is expected that the effective temperature is slightly smaller than volume-average temperature due to higher importance of the periphery region of fuel pellet. On the other hand, the  $k_{inf}$  of volume-average temperature

is higher than that of effective temperature. This is because of fuel Doppler effect as the volume-average temperature is higher than effective temperature. The multiplication factor difference between reference and effective values is negligible within the uncertainty of 6.5 pcm. That is, the reactivity is preserved with the use of effective temperature.

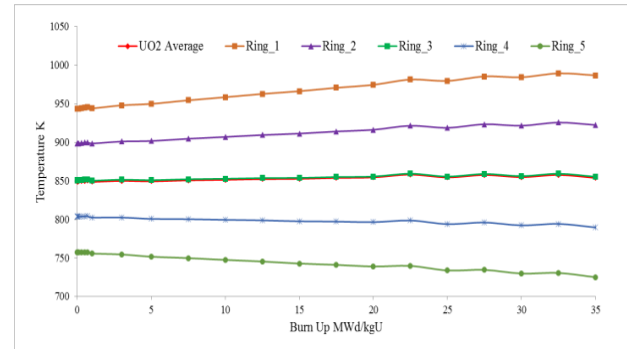


Fig. 7: Ring-wise and volume-average temperatures as a function of burnup.

Table 2: Burnup-dependent multiplication factors at different temperatures

Burnup (MWd/kgU)	$k_{inf}$ (reference)	$k_{inf}$ ( $T_{eff}$ )	Effective T (K)	Difference* (pcm)	$k_{inf}$ ( $T_{avg}$ )	Average T (K)	Difference ** (pcm)
0	1.150166	1.150173	839.50	-0.53	1.149783	849.25	28.96
10	1.016021	1.016023	839.70	-0.09	1.015740	851.41	27.23
20	0.964887	0.964875	845.75	1.30	0.964546	854.55	36.64
30	0.832647	0.832630	839.71	2.44	0.832231	854.88	60.03

\* Difference between  $k_{inf}$  ( $T_{eff}$ ) and  $k_{inf}$  (reference), \*\* Difference between  $k_{inf}$  ( $T_{avg}$ ) and  $k_{inf}$  (reference)

## 5. Conclusion

In this paper, the FEM code, coupled with Serpent calculation, is successfully developed to estimate the detailed burnup-dependent temperature distribution of newly proposed CSBA fuel design. It is found that the average fuel temperature of the CSBA pellet is almost constant and lower than that of conventional PWR pellet. The effective temperature is also estimated using the detailed temperature profile. It is expected that the effective temperature is lower than volume-average temperature, due to higher importance of periphery region. The future work is dedicated to evaluate the temperature of other CSBA fuel design.

## REFERENCES

[1] Goltsev, A.O., Davidenko, V.D., Tsubulsky, V.F., Lekomtsev, A.A., 2000. Computational problems in the calculation of temperature effects for heterogeneous nuclear reactor unit cells. *Annals of Nuclear Energy* 27 (2), 175-183.  
[2] Rowlands, G., 1962. Resonance absorption and non-uniform temperature distributions. *Journal of Nuclear Energy, Parts A and B* 16, 235.

[3] Y.M. Syukri, K. Yonghee, Centrally-shielded burnable absorber for LWR fuel, ICAPP April 24-28 2017.  
[4] J. Leppänen, M. Pusa, T. Viitanen, V. Valtavirta and T. Kaltiaisenaho, "The Serpent Monte Carlo Code: Status, Development and Applications in 2013," *Ann. Nucl. Energy*. 2015 Aug; 82:142-150.  
[5] P. Nithiarasu, R.W. Lewis and K.N. Seetharamu, *Fundamentals of the Finite Element Method for Heat and Mass Transfer*, Second Edition, John Wiley & Sons Ltd, p 150-153